

BUCKLING OPTIMIZATION OF UNSYMMETRICALLY LAMINATED PLATES UNDER TRANSVERSE LOADS

Hsuan-Teh Hu and Zhong-Zhi Chen

*Department of Civil Engineering, National Cheng Kung University
Tainan, Taiwan 701, R.O.C.*

SUMMARY: The critical buckling loads of unsymmetrically laminated rectangular plates with a given material system and subjected to combined lateral and inplane loads are maximized against fiber orientations by using a sequential linear programming method together with a simple move-limit strategy. Significant influence of plate aspect ratios, central circular cutouts, lateral loads and end conditions on the optimal fiber orientations and the associated optimal buckling loads of unsymmetrically laminated plates has been shown through this investigation.

KEYWORDS: buckling, optimization, unsymmetrically laminated plates

INTRODUCTION

The composite laminate plates in service are commonly subjected to compressive forces which may cause buckling. Hence, structural instability becomes a major concern in safe and reliable design of the composite plates. The buckling resistance of composite laminate plates depends on end conditions, ply orientations [1-3], and geometric variables such as aspect ratios, thicknesses and cutouts [2,4]. Therefore, for composite plates with a given material system, geometric shape, thickness and end condition, the proper selection of appropriate lamination to realize the maximum buckling resistance of the plates becomes a crucial problem. Among various optimization schemes, the method of sequential linear programming has been successfully applied to many large scale structural problems [5,6].

In this study, the critical buckling loads of unsymmetrically laminated plates subjected to inplane and transverse loads are calculated by the bifurcation buckling analysis implemented in the ABAQUS finite element program [7]. Then, buckling optimization of unsymmetrically laminated plates with respect to fiber orientations is performed by using a sequential linear programming method together with a simple move-limit strategy. In the paper, the buckling analysis, the constitutive equations for fiber-composite laminate and the optimization method are briefly reviewed first. Then the influence of plate aspect ratios, central circular cutouts, lateral loads and end conditions on the optimal fiber orientations and the associated optimal buckling loads of unsymmetrically laminated composite plates is presented.

BIFURCATION BUCKLING ANALYSIS

In the finite-element analysis, a set of nonlinear equations results in the incremental form:

$$[K_t]d\{u\} = d\{p\} \quad (1)$$

where $[K_t]$ is the tangent stiffness matrix, $d\{u\}$ the incremental nodal displacement vector and $d\{p\}$ the incremental nodal force vector. When the structural deformation is small, the nonlinear theory leads to the same critical load as the linear theory. The linearized formulation then gives rise to a tangent stiffness matrix in the following expression:

$$[K_t] = [K_L] + [K_\sigma] \quad (2)$$

where $[K_L]$ is a linear stiffness matrix and $[K_\sigma]$ a stress stiffness matrix. If a stress stiffness matrix $[K_\sigma]_{\text{ref}}$ is generated according to a reference load $\{p\}_{\text{ref}}$, for another load level $\{p\}$ with λ a scalar multiplier, we have

$$\{p\} = \lambda\{p\}_{\text{ref}}, \quad [K_\sigma] = \lambda[K_\sigma]_{\text{ref}} \quad (3)$$

When buckling occurs, the external loads do not change, i.e., $d\{p\} = 0$. Then the solution for the linearized buckling problem may be determined from the following eigenvalue equation:

$$([K_L] + \lambda_{\text{cr}}[K_\sigma]_{\text{ref}}) d\{u\} = \{0\} \quad (4)$$

where λ_{cr} is an eigenvalue and $d\{u\}$ becomes the eigenvector defining the buckling mode. The critical load $\{p\}_{\text{cr}}$ can be obtained from $\{p\}_{\text{cr}} = \lambda_{\text{cr}}\{p\}_{\text{ref}}$.

CONSTITUTIVE MATRIX FOR FIBER-COMPOSITE LAMINATE

The laminate plates are modeled by eight-node isoparametric laminate shell elements with six degrees of freedom per node. The formulation of the shell element allows transverse shear deformation [7]. For fiber-composite laminate materials, the stress-strain relations for a lamina in the material coordinates (1,2,3) at an element integration point can be written as

$$\begin{aligned} \{\sigma'\} &= [Q_1']\{\varepsilon'\}, & \{\tau'\} &= [Q_2']\{\gamma'\} \end{aligned} \quad (5)$$

$$[Q_1'] = \begin{bmatrix} \frac{E_{11}}{1-\nu_{12}\nu_{21}} & \frac{\nu_{12}E_{22}}{1-\nu_{12}\nu_{21}} & 0 \\ \frac{\nu_{21}E_{11}}{1-\nu_{12}\nu_{21}} & \frac{E_{22}}{1-\nu_{12}\nu_{21}} & 0 \\ 0 & 0 & G_{12} \end{bmatrix}, \quad [Q_2'] = \begin{bmatrix} \alpha_1 G_{13} & 0 \\ 0 & \alpha_2 G_{23} \end{bmatrix} \quad (6)$$

where $\{\sigma'\} = \{\sigma_1, \sigma_2, \tau_{12}\}^T$, $\{\tau'\} = \{\tau_{13}, \tau_{23}\}^T$, $\{\varepsilon'\} = \{\varepsilon_1, \varepsilon_2, \gamma_{12}\}^T$, $\{\gamma'\} = \{\gamma_{13}, \gamma_{23}\}^T$. The α_1 and α_2 are shear correction factors calculated by assuming that the transverse shear energy through the thickness of laminate is equal to that of the case of unidirectional bending [7]. The constitutive equations for the lamina in the element coordinates (x,y,z) then become

$$\{\sigma\} = [Q_1]\{\varepsilon\}, \quad [Q_1] = [T_1]^T [Q_1'] [T_1] \quad (7)$$

$$\{\tau\} = [Q_2]\{\gamma\}, \quad [Q_2] = [T_2]^T [Q_2'] [T_2] \quad (8)$$

$$[T_1] = \begin{bmatrix} \cos^2 \theta & \sin^2 \theta & \sin \theta \cos \theta \\ \sin^2 \theta & \cos^2 \theta & -\sin \theta \cos \theta \\ -2 \sin \theta \cos \theta & 2 \sin \theta \cos \theta & \cos^2 \theta - \sin^2 \theta \end{bmatrix}, [T_2] = \begin{bmatrix} \cos \theta & \sin \theta \\ -\sin \theta & \cos \theta \end{bmatrix} \quad (9)$$

where $\{\sigma\} = \{\sigma_x, \sigma_y, \tau_{xy}\}^T$, $\{\tau\} = \{\tau_{xz}, \tau_{yz}\}^T$, $\{\varepsilon\} = \{\varepsilon_x, \varepsilon_y, \gamma_{xy}\}^T$, $\{\gamma\} = \{\gamma_{xz}, \gamma_{yz}\}^T$, and fiber angle θ is measured counterclockwise from the element local x-axis to the material 1-axis. Let $\{\varepsilon_0\} = \{\varepsilon_{x0}, \varepsilon_{y0}, \gamma_{xy0}\}^T$ be the in-plane strains at the mid-surface of the laminate section, $\{\kappa\} = \{\kappa_x, \kappa_y, \kappa_{xy}\}^T$ the curvatures, and h the total thickness of the section. If there are n layers in the layup, the stress resultants, $\{N\} = \{N_x, N_y, N_{xy}\}^T$, $\{M\} = \{M_x, M_y, M_{xy}\}^T$ and $\{V\} = \{V_x, V_y\}^T$, can be defined as

$$\begin{Bmatrix} \{N\} \\ \{M\} \\ \{V\} \end{Bmatrix} = \int_{-h/2}^{h/2} \begin{Bmatrix} \{\sigma\} \\ z\{\sigma\} \\ \{\tau\} \end{Bmatrix} dz = \sum_{j=1}^n \begin{bmatrix} (z_{jt} - z_{jb})[Q_1] & \frac{1}{2}(z_{jt}^2 - z_{jb}^2)[Q_1] & [0] \\ \frac{1}{2}(z_{jt}^2 - z_{jb}^2)[Q_1] & \frac{1}{3}(z_{jt}^3 - z_{jb}^3)[Q_1] & [0] \\ [0]^T & [0]^T & (z_{jt} - z_{jb})[Q_2] \end{bmatrix} \begin{Bmatrix} \{\varepsilon_0\} \\ \{\kappa\} \\ \{\gamma\} \end{Bmatrix} \quad (10)$$

where z_{jt} and z_{jb} are the distance from the mid-surface of the section to the top and the bottom of the j -th layer. The $[0]$ is a 3 by 2 matrix with all the coefficients equal to zero.

SEQUENTIAL LINEAR PROGRAMMING

A general optimization problem may be defined as the following:

$$\text{Maximize: } f(\underline{x}) \quad (11.a)$$

$$\text{Subjected to: } g_i(\underline{x}) \leq 0, \quad i = 1, \dots, r \quad (11.b)$$

$$h_j(\underline{x}) = 0, \quad j = r+1, \dots, m \quad (11.c)$$

$$p_k \leq x_k \leq q_k, \quad k = 1, \dots, n \quad (11.d)$$

where $\underline{x} = \{x_1, x_2, \dots, x_n\}^T$ is a vector of design variables, $f(\underline{x})$ is an objective function, $g_i(\underline{x})$ are inequality constraints, and $h_j(\underline{x})$ are equality constraints. The p_k and q_k are lower and upper limits of the variable x_k . For the optimization problem of Eqs. (11.a)-(11.d), a linearized problem may be constructed by approximating the nonlinear functions at a current solution point, $\underline{x}_0 = \{x_{01}, x_{02}, \dots, x_{0n}\}^T$, in a first-order Taylor series expansion as follows

$$\text{Maximize: } f(\underline{x}) \approx f(\underline{x}_0) + \nabla f(\underline{x}_0)^T \delta \underline{x} \quad (12.a)$$

$$\text{Subjected to: } g_i(\underline{x}) \approx g_i(\underline{x}_0) + \nabla g_i(\underline{x}_0)^T \delta \underline{x} \leq 0, \quad i = 1, \dots, r \quad (12.b)$$

$$h_j(\underline{x}) \approx h_j(\underline{x}_0) + \nabla h_j(\underline{x}_0)^T \delta \underline{x} = 0, \quad j = r+1, \dots, m \quad (12.c)$$

$$p_k \leq x_k \leq q_k, \quad k = 1, \dots, n \quad (12.d)$$

where $\delta \underline{x} = \{x_1 - x_{01}, x_2 - x_{02}, \dots, x_n - x_{0n}\}^T$. It is clear that the above expressions represent a linear programming problem and the solution can be obtained by the simplex method [8]. After obtaining an approximate solution for Eqs. (12.a)-(12.d), say \underline{x}_1 , we can linearize the original problem at \underline{x}_1 and solve the new linear programming problem. The process is repeated until a precise solution is achieved. This approach is referred to as sequential linear programming [5,6]. Although the procedure for sequential linear programming is simple, the optimum solution for the approximated linear problem may violate the constraint conditions of the original optimization problem. In addition, if the true optimum solution of a nonlinear problem appears between two constraint intersections, a straightforward successive

linearization may lead to an oscillation of the solution between the widely separated values. Difficulties in dealing with such problems may be avoided by imposing a “move limit” [5,6] on the linear approximation, which is a set of box-like admissible constraints placed on the range of $\delta\bar{x}$. The move limit should gradually approach to zero as the iterative process of the sequential linear programming continues.

RESULTS OF THE OPTIMIZATION ANALYSIS

Laminate Plates with Simply Supported Edges

In this section rectangular composite laminate plates subjected to uniaxial compressive force N per unit length applied at the edges normal to the x direction as shown in Fig. 1(a) are analyzed. The width of the plates, b , is 10 cm while the length, a , is varied between 5 cm and 30 cm. The edges of the plates are all simply supported, which prevents out of plane displacement w but allows some inplane u and v movements. In this regard, all the points on the right edge of the plates are enforced to displace the same amount u in the x direction, while all the points on the upper edge of the plates are enforced to displace the same amount v in the y direction. The thickness of each ply is 0.125 mm. The laminate lay-ups of the plates are $[\pm\theta/90/0]_{2s}$ (symmetric lay-up) and $[(\pm\theta_1/90/0)_2]/(0/90/\mp\theta_2)_2$ (asymmetric lay-up). The lamina consists of Graphite/Epoxy with material constitutive properties taken from Crawley [9], which are $E_{11} = 128$ GPa, $E_{22} = 11$ GPa, $\nu_{12} = 0.25$, $G_{12} = G_{13} = 4.48$ GPa, $G_{23} = 1.53$ GPa.

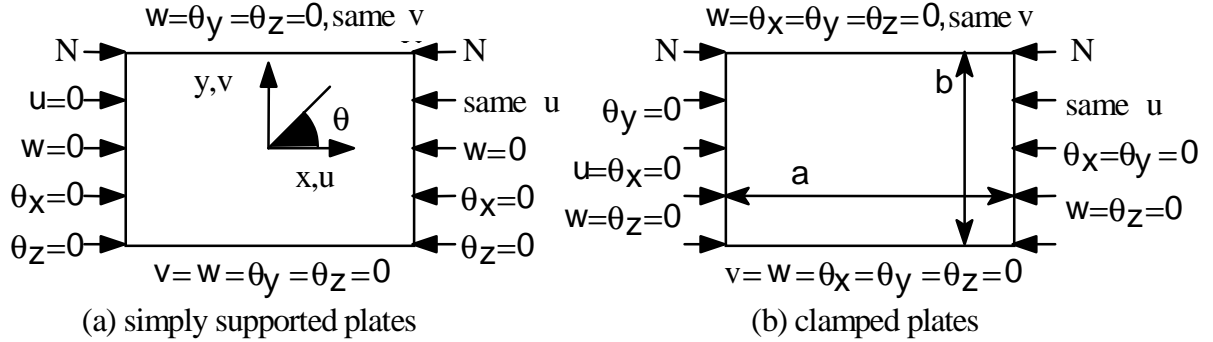


Fig. 1: Rectangular composite laminate plates with different edge conditions

Based on the sequential linear programming method, in each iteration the current linearized optimization problem for symmetrically laminated composite plates becomes:

$$\text{Maximize: } N_{cr}(\theta) \approx N_{cr}(\theta_o) + (\theta - \theta_o) \left. \frac{\partial N_{cr}}{\partial \theta} \right|_{\theta=\theta_o} \quad (13.a)$$

$$\text{Subjected to: } 0^\circ \leq \theta \leq 90^\circ \quad (13.b)$$

$$-R \times Q \times 0.5^s \leq (\theta - \theta_o) \leq R \times Q \times 0.5^s \quad (13.c)$$

where N_{cr} is the critical buckling load. The θ_o is a solution obtained in the previous iteration. The R and Q in Eq. (13.c) are the size and the reduction rate of the move limit. In the present study, the values of R and Q are selected to be 10° and $0.9^{(M-1)}$, where M is a current iteration number. To control the oscillation of the solution, a parameter 0.5^s is introduced in the move limit, where s is the number of oscillations of the derivative $\partial N_{cr}/\partial \theta$ that has taken place before the current iteration. The value of s increases by 1 if the sign of $\partial N_{cr}/\partial \theta$ changes. Whenever oscillation of the solution occurs, the range of the move limit is reduced to half of

its current value. This expedites the solution convergent rate very rapidly. The $\partial N_{cr}/\partial\theta$ term in Eq. (13.a) may be approximated by using a forward finite-difference method with the following form:

$$\frac{\partial N_{cr}}{\partial\theta} \approx \frac{N_{cr}(\theta_o + \Delta\theta) - N_{cr}(\theta_o)}{\Delta\theta} \quad (14)$$

Hence, to determine the value of $\partial N_{cr}/\partial\theta$ numerically, two bifurcation buckling analyses to compute $N_{cr}(\theta_o)$ and $N_{cr}(\theta_o+\Delta\theta)$ are needed in each iteration. In this study, the value of $\Delta\theta$ is selected to be 1° in most iterations.

The linearized optimization problem for asymmetrically laminated plates can be written as:

$$\begin{aligned} \text{Maximize: } \quad N_{cr}(\theta_1, \theta_2) \approx N_{cr}(\theta_{o1}, \theta_{o2}) &+ (\theta_1 - \theta_{o1}) \left. \frac{\partial N_{cr}}{\partial\theta_1} \right|_{\theta_1=\theta_{o1}, \theta_2=\theta_{o2}} \\ &+ (\theta_2 - \theta_{o2}) \left. \frac{\partial N_{cr}}{\partial\theta_2} \right|_{\theta_1=\theta_{o1}, \theta_2=\theta_{o2}} \end{aligned} \quad (15.a)$$

$$\text{Subjected to: } 0^\circ \leq \theta_1 \leq 90^\circ \quad (15.b)$$

$$0^\circ \leq \theta_2 \leq 90^\circ \quad (15.c)$$

$$-R_1 \times Q_1 \times 0.5^{s_1} \leq (\theta_1 - \theta_{o1}) \leq R_1 \times Q_1 \times 0.5^{s_1} \quad (15.d)$$

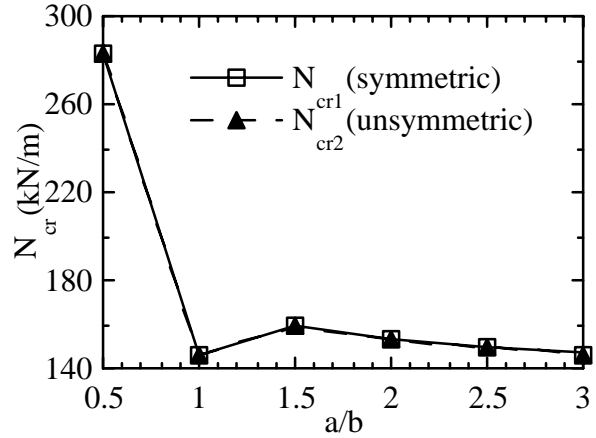
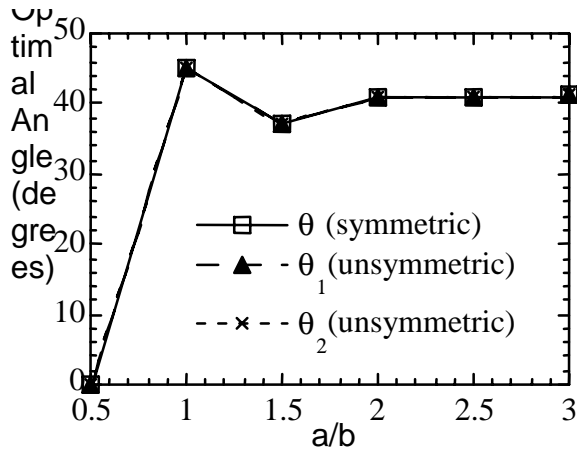
$$-R_2 \times Q_2 \times 0.5^{s_2} \leq (\theta_2 - \theta_{o2}) \leq R_2 \times Q_2 \times 0.5^{s_2} \quad (15.e)$$

where $(\theta_{o1}, \theta_{o2})$ is a solution obtained in the previous iteration. The values of R_1 and R_2 are selected to be 20° and Q_1 and Q_2 are selected to be $0.9^{(M-1)}$. Again, s_1 and s_2 are the numbers of oscillations of the derivatives $\partial N_{cr}/\partial\theta_1$ and $\partial N_{cr}/\partial\theta_2$ that have taken place before the current iteration, respectively. The $\partial N_{cr}/\partial\theta_1$ and $\partial N_{cr}/\partial\theta_2$ terms in eq. (15.a) may be approximated by forward finite-difference expressions as follows:

$$\frac{\partial N_{cr}}{\partial\theta_1} \approx \frac{N_{cr}(\theta_{o1} + \Delta\theta, \theta_{o2}) - N_{cr}(\theta_{o1}, \theta_{o2})}{\Delta\theta} \quad (16.a)$$

$$\frac{\partial N_{cr}}{\partial\theta_2} \approx \frac{N_{cr}(\theta_{o1}, \theta_{o2} + \Delta\theta) - N_{cr}(\theta_{o1}, \theta_{o2})}{\Delta\theta} \quad (16.b)$$

Hence, three bifurcation buckling analyses to compute $N_{cr}(\theta_{o1}+\Delta\theta, \theta_{o2})$, $N_{cr}(\theta_{o1}, \theta_{o2}+\Delta\theta)$ and $N_{cr}(\theta_{o1}, \theta_{o2})$ are needed in each iteration. Again, the value of $\Delta\theta$ is selected to be 1° in most iterations. For each case studied, several different initial guesses of fiber angles are selected to make sure that they all converge to the same global maximum solution.



(a) Aspect ratio a/b vs. optimal fiber angle

(b) Aspect ratio a/b vs. critical load

Fig. 2: Effect of plate aspect ratios on buckling optimization of $[\pm\theta/90/0]_{2s}$ and $[(\pm\theta_1/90/0)_2]/(0/90/\mp\theta_2)_2$ rectangular composite plates with simply supported edges and subjected to inplane force

Figure 2 shows the optimal fiber angle and the associated optimal buckling load N_{cr} with respect to plate aspect ratio a/b for $[\pm\theta/90/0]_{2s}$ and $[(\pm\theta_1/90/0)_2]/(0/90/\mp\theta_2)_2$ rectangular composite plates. From the figure we can see that the optimal fiber angles and optimal buckling loads attenuate to constant values when the plate aspect ratios are large. It is not surprising to find that the results of optimization for plates with symmetric and unsymmetric lay-ups are all the same. This is because when buckling occurs, there is no preference for plates to buckle up or down. Thus, for composite plates under inplane loading conditions, there is no benefit to employ the unsymmetric laminate lay-up.

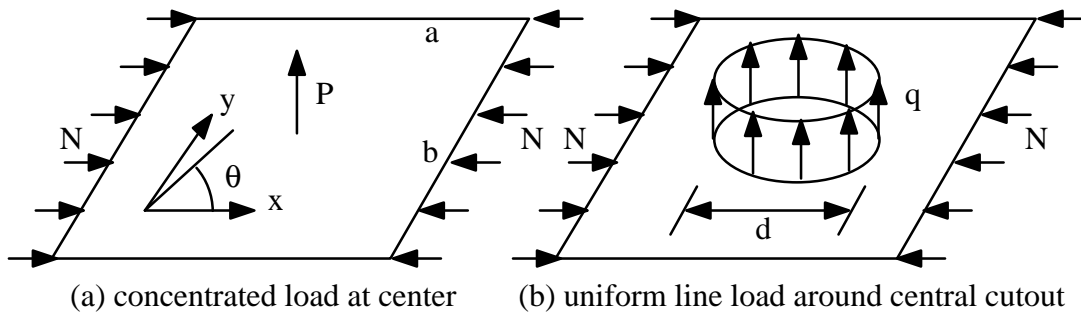
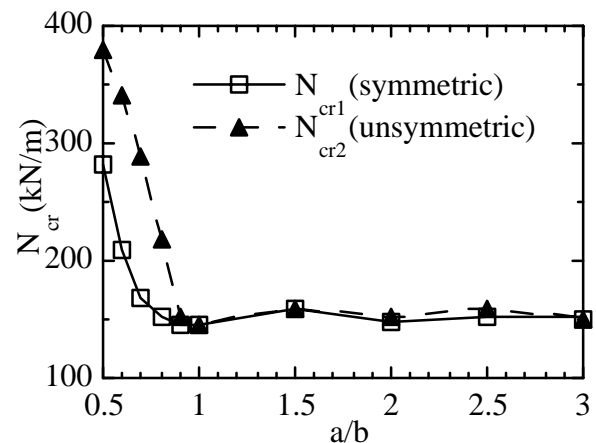
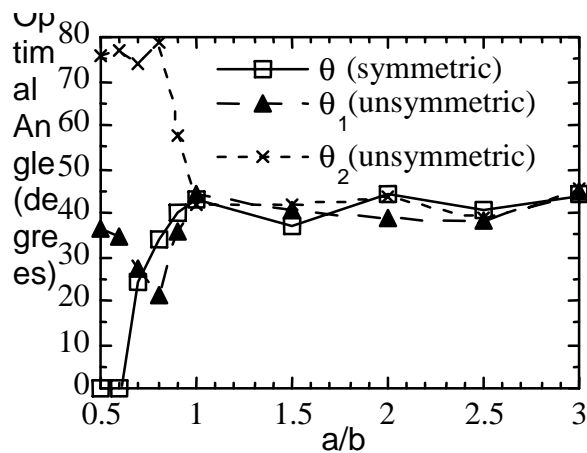


Fig. 3: Rectangular plates with combined inplane and lateral forces



(a) Aspect ratio a/b vs. optimal fiber angle

(b) Aspect ratio a/b vs. critical load

Fig. 4: Effect of plate aspect ratios on buckling optimization of $[\pm\theta/90/\theta]_2$ and $[(\pm\theta_1/90/0)_2]/(0/90/\mp\theta_2)_2$ rectangular composite plates with simply supported edges and subjected to combined inplane and lateral forces

In addition to inplane forces, the composite plates in service may also be subjected to lateral forces. As another example, composite plates similar to previous ones but with an additional lateral concentrated load P acting at the center of the plates as shown in Fig. 3(a) are analyzed. In the analysis, the ratio $P/(Nb) = 0.5$ is used. Figure 4 shows the optimal fiber angle and the associated optimal buckling load N_{cr} with respect to plate aspect ratio a/b for $[\pm\theta/90/0]_{2s}$ and $[(\pm\theta_1/90/0)_2]/(0/90/\mp\theta_2)_2$ rectangular composite plates. The figure shows that when the plate aspect ratio is large (say $a/b > 1$), the results of optimization for plates with unsymmetric lay-ups are very similar to those for plates with symmetric lay-ups. In addition, as a/b ratio increases, the optimal fiber angles and optimal buckling loads gradually approach constant values. However, when the plate aspect ratio is small (say $a/b < 1$), the optimal fiber angles of plates with asymmetric lay-ups are quite different from those of plates with symmetric lay-ups. In addition the optimal buckling loads of the former plates are much higher than those of the latter plates. By comparing with the plates with symmetric layups, the implementation of unsymmetric layups in some cases (say $a/b = 0.7$) may increase the optimal buckling loads of plates by 70%. It is noted [10] that when the plate aspect ratio is small the optimal buckling modes of unsymmetrically laminated plates are quite different from those of symmetrically laminated plates. However, when the plate aspect ratio is large, the optimal buckling modes of unsymmetrically laminated plates are very similar to those of symmetrically laminated plates. Also, as a/b ratio increases, the optimal buckling modes of plates have more waves in x direction.

Laminate Plates with Clamped Edges

In order to find the effect of boundary conditions on the results of optimization, the composite plates subjected to combined inplane and lateral forces in previous section are analyzed again, however, with all edges clamped as shown in Fig. 1(b). Figure 5 shows the optimal fiber angle and the associated optimal buckling load N_{cr} with respect to plate aspect ratio a/b for $[\pm\theta/90/0]_{2s}$ and $[(\pm\theta_1/90/0)_2]/(0/90/\mp\theta_2)_2$ rectangular composite plates with clamped edges. Form the figure we can observe that except plates with small aspect ratio (say a/b around 0.5), the results of optimization for plates with unsymmetric lay-ups are very different from those for plates with symmetric lay-ups. In addition, when $a/b \geq 1$, the optimal buckling loads of plates with unsymmetric lay-ups are higher than those of plates with symmetric lay-ups by up to 20%. It is also known [10] that the optimal buckling modes for symmetrically and unsymmetrically laminated plates with clamped edges and under optimal fiber orientation are very similar. Again, as a/b ratio increases, the optimal buckling modes of plates have more waves in x direction.

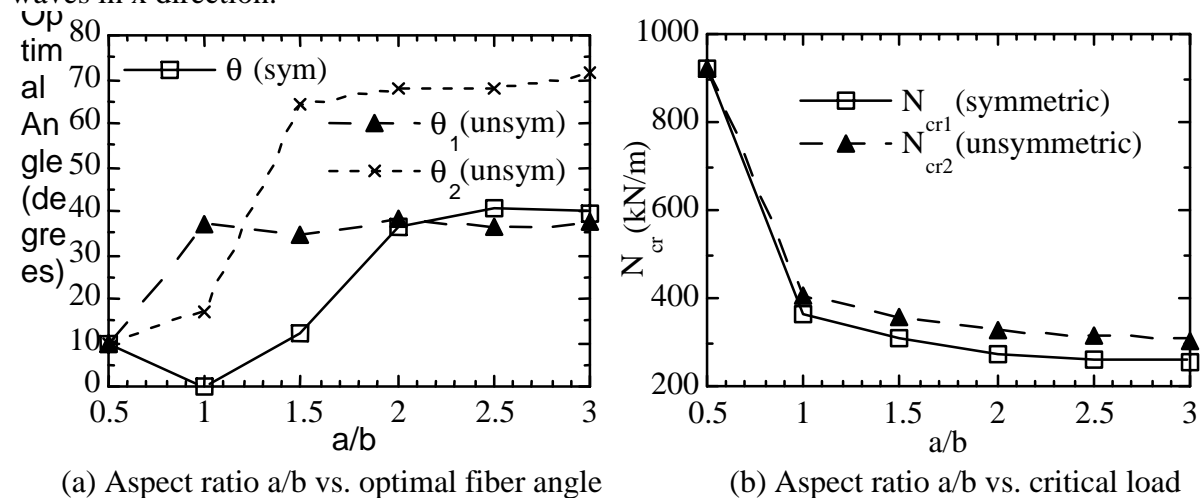


Fig. 5: Effect of plate aspect ratios on buckling optimization of $[\pm\theta/90/0]_{2s}$ and $[(\pm\theta_1/90/0)_2]/(0/90/\mp\theta_2)_2$ rectangular composite plates with clamped edges and subjected to combined inplane and lateral forces

Laminate Plates with Various Central Circular Cutouts and with Simply Supported Edges

In this section $[\pm\theta/90/0]_{2s}$ and $[(\pm\theta_1/90/0)_2]/(0/90/\mp\theta_2)_2$ rectangular composite laminate plates with central circular cutouts and subjected to combined in-plane force and lateral force (a uniform line load of intensity q) as shown in Fig. 3(b) are analyzed. The edges of the plates are all simply supported. The width of the plates, b , is 10 cm, the length of the plates, a , is 7 cm, the diameter of the hole, d , varies from 0 to 5 cm, and the ratio $q\pi d/(Nb) = 0.5$ is used. Figure 6 shows the optimal fiber angle and the associated optimal buckling load N_{cr} with respect to the ratio d/b for symmetric and unsymmetric rectangular composite plates. The figure shows that the results of optimization for plates with unsymmetric lay-ups are very different from those for plates with symmetric lay-ups. In addition, the optimal buckling loads of the former plates are much higher than those of the latter plates. In some cases (say $d/b = 0.5$), the implementation of unsymmetric lay-ups may increase the buckling loads of the plates by 300%. For plates with symmetric lay-ups, the optimal buckling load (say $d/b < 0.4$) first decreases with the increasing of d/b ratio then it (say $d/b > 0.4$) increases with the increase of the cutout sizes. For plates with unsymmetric lay-ups, the optimal buckling load increases with the increase of the sizes of cutouts. This phenomenon is quite different from our intuition that introducing a large hole into a plate can cause a reduction in the buckling load of the plate. However, past research did show (numerically and experimentally) that introducing a hole into an isotropic plate or a composite plate does not always reduce the buckling load and, in some instances, may increase its buckling load [4,11]. This is because that the buckling load of a plate is not only influenced by cutout, but also influenced by material orthotropy, end condition, and plate geometry. It is also known [10] that the buckling modes of plates with unsymmetric lay-ups under optimal conditions are quite different from those of plates with symmetric lay-ups. Generally, the buckling modes of plates with unsymmetric lay-ups have more waves in both x and y directions.

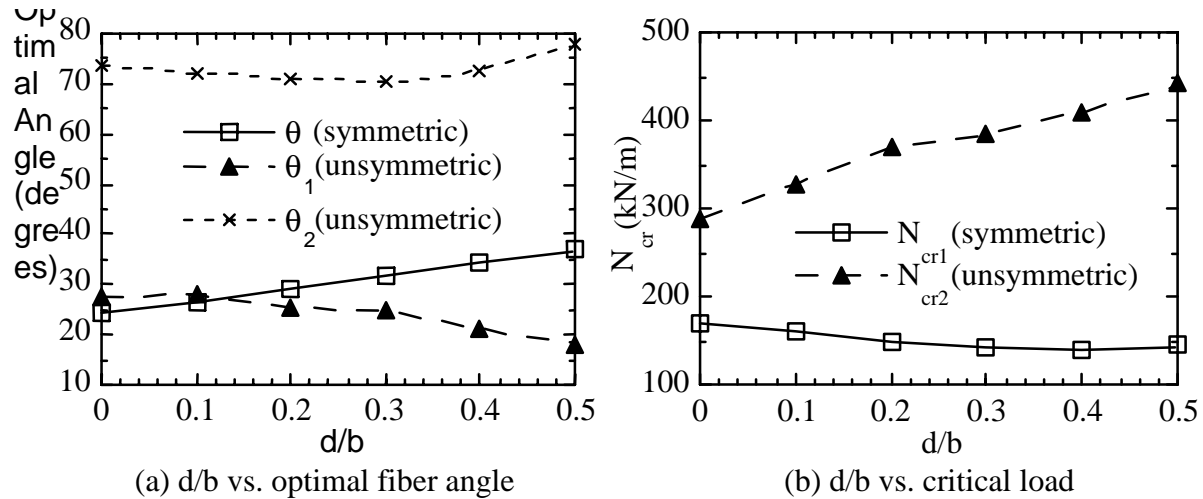


Fig. 6: Effect of cutout size on buckling optimization of $[\pm\theta/90/0]_{2s}$ and $[(\pm\theta_1/90/0)_2]/(0/90/\mp\theta_2)_2$ rectangular composite plates with simply supported edges and subjected to combined inplane and lateral forces ($a/b = 0.7$)

Laminate Plates with Various Central Circular Cutouts and with Clamped Edges

In this section, the composite laminate plates with central circular cutouts similar to those in previous section are analyzed again, however, with all edges changed to clamped conditions and a/b ratio changed to 1.5. The width b of the plates is still 10 cm, the cutout size varies between 2 cm and 8 cm, and the ratio $q\pi d/(Nb) = 0.5$ is still kept in the analysis. Figure 7 shows the optimal fiber angle and the associated optimal buckling load N_{cr} with respect to the ratio d/b for $[\pm\theta/90/0]_{2s}$ and $[(\pm\theta_1/90/0)_2]/(0/90/\pm\theta_2)_2$ rectangular composite plates. Figure 7(a) shows that the optimal fiber angles for plates with asymmetric lay-ups are very different from those for plates with symmetric lay-ups. Figure 7(b) shows that the optimal buckling loads of the former plates are generally higher than those of the latter plates. In some cases (say $d/b < 0.2$), the implementation of unsymmetric lay-ups may increase the buckling loads of the plates by 15%. For plates with either symmetric or asymmetric lay-up, the optimal buckling load seems to be a second-order function of the cutout size. It is also known [10] that when $d/b > 0.2$, the buckling modes of plates with unsymmetric lay-ups under optimal conditions are quite different from those of plates with symmetric lay-ups. Nevertheless, for both types of plates, when the cutout sizes are large, the buckling modes are more locally around the cutout areas.

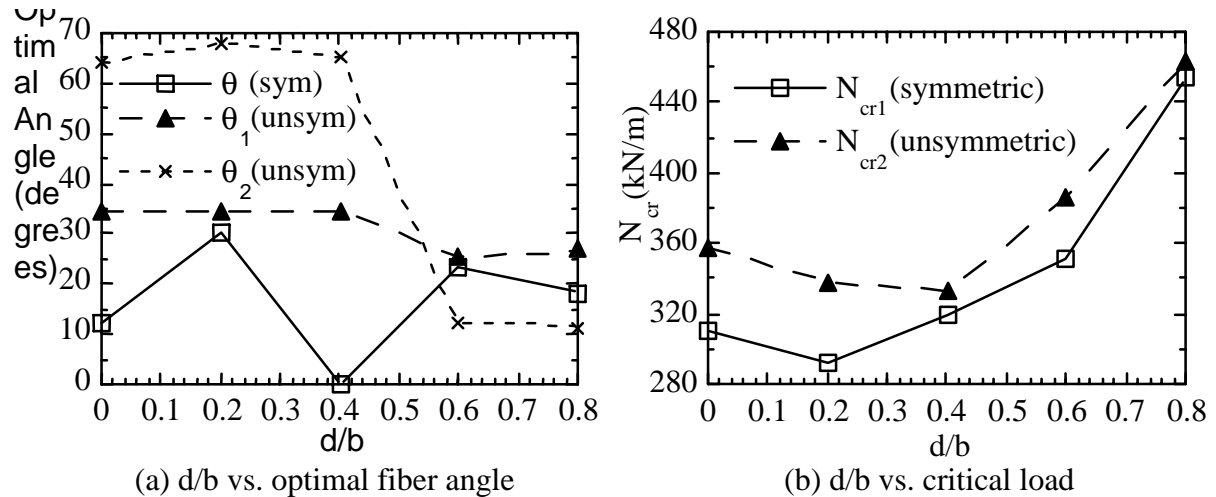


Fig. 7: Effect of cutout size on buckling optimization of $[\pm\theta/90/0]_{2s}$ and $[(\pm\theta_1/90/0)_2]/(0/90/\pm\theta_2)_2$ rectangular composite plates with clamped edges and subjected to combined inplane and lateral forces ($a/b = 1.5$)

CONCLUSIONS

In the process of sequential linear programming, most optimal results are obtained within 13 iterations, and the results are all verified by choosing different initial guesses. Hence, as a general conclusion, the sequential linear programming is efficient and stable to solve nonlinear optimization problems. For the optimal buckling analysis of uniaxially compressed symmetric $[\pm\theta/90/0]_{2s}$ and unsymmetric $[(\pm\theta_1/90/0)_2]/(0/90/\mp\theta_2)_2$ laminated plates with various plate aspect ratios, circular cutouts and end conditions, the following conclusions may be drawn:

1. For composite plates under inplane loading conditions, there is no benefit to be derived from employing an unsymmetric laminate layup.
2. For composite plates with simply supported edges and subjected to combined inplane and lateral loads, it is beneficial to employ the unsymmetric laminate lay-ups when the plate

aspect ratio is small (say $a/b < 1$).

3. For composite plates with clamped edges and subjected to combined inplane and lateral loads, the adoption of unsymmetric laminate design is beneficial when the plate aspect ratio is large (say $a/b > 1$).
4. For composite plates with a central circular cutout and subjected to combined inplane and lateral loads, the use of unsymmetric laminate layups is recommended. The optimal buckling loads of these plates in some cases (say plates with clamped edges) may increase with the increasing of cutout sizes. Hence, it is possible to tailor the cutout size and fiber angle to increase the buckling loads of these plates beyond those of corresponding plates without cutouts.

In this paper, bifurcation buckling analysis is carried out based on the assumption that the composite laminate material behaves linearly. For low aspect ratio plates and for plates with large cutouts, the stresses in the laminates may exceed the elastic range and these laminates are probably driven by compression strength failure in stead of buckling. In these cases, buckling analyses of composite plates based on nonlinear material properties are recommended [12].

REFERENCES

1. Hirano, Y., "Optimum Design of Laminated Plates under Axial Compression", *AIAA Journal*, Vol. 17, 1979, pp. 1017-1019.
2. Leissa, A.W., *Buckling of Laminated Composite Plates and Shell Panels*. AFWAL-TR-85-3069, Flight Dynamics Laboratory, Air Force Wright Aeronautical Laboratories, Wright-Patterson Air Force Base, Ohio, 1985.
3. Muc, A., "Optimal Fibre Orientation for Simply-Supported Angle-Ply Plates under Biaxial Compression", *Composite Structures*, Vol. 9, 1988, pp. 161-172.
4. Nemeth, M.P., "Buckling Behavior of Compression-Loaded Symmetrically Laminated Angle-Ply Plates with Holes", *AIAA Journal*, Vol. 26, 1988, pp. 330-336.
5. Zienkiewicz, O.C. and Champbell, J.S., "Shape Optimization and Sequential Linear Programming", *Optimum Structural Design, Theory and Applications*, edited by Gallagher, R.H. and Zienkiewicz, O.C., Wiley, New York, 1973, pp. 109-126.
6. Vanderplaats, G.N., *Numerical Optimization Techniques for Engineering Design with Applications*, Chapter 6, McGraw-Hill, New York. 1984.
7. Hibbitt, Karlsson & Sorensen, Inc., *ABAQUS User and Theory Manuals Version 5.7*, Providence, Rhode Island, 1998.
8. Kolman, B. and Beck, R.E., *Elementary Linear Programming with Applications*, Chapter 2, Academic Press, Orlando, 1980.
9. Crawley, E.F., "The Natural Modes of Graphite/Eever Plates and Shells", *Journal of Composite Materials*, Vol. 13, 1979, pp. 195-205.

10. Chen, Z.-Z., *Buckling Optimization of Symmetric and Unsymmetric Laminate Plates Subjected to Combined Inplane and Lateral Loads*, M.S. Thesis, Department of Civil Engineering, National Cheng Kung University, Tainan, Taiwan, R.O.C., 1995.
11. Ritchie, D. and Rhoades, J., "Buckling and Postbuckling Behavior of Plates with Holes", *Aeronautical Quarterly*, Vol. 26, 1975, pp. 281-296.
12. Hu, H.-T., "Buckling Analyses of Fiber Composite Laminate Plates with Material Nonlinearity", *Finite Elements in Analysis and Design*, Vol. 19, 1995, pp. 169-179.